

Supporting information

Origin of electrochemical cycling stability induced by calcination temperature for cobalt-free nickel-rich cathodes

Chenxi Song, Yaoyu Ren*, Lin Gu, Qingyun Zhang, Yang Lu, Yang Shen*

C. Song, Prof. Y. Ren, Prof. L. Gu, Prof. Y. Shen

State Key Laboratory of New Ceramics and Fine Processing

School of Materials Science and Engineering

Tsinghua University, Beijing 100084, China

E-mail: renyaoyu@mail.tsinghua.edu.cn; shyang_mse@mail.tsinghua.edu.cn

Q. Zhang, Y. Lu

China North Vehicle Research Institute, Beijing 100072, China

Materials Synthesis

The Co-free Ni-rich $\text{LiNi}_{0.9}\text{Mn}_{0.1}\text{O}_2$ cathodes were prepared through a solid-state calcination process. The $\text{Ni}_{0.9}\text{Mn}_{0.1}(\text{OH})_2$ precursor (YouyanTech Co., Ltd.) was ground with $\text{LiOH}\cdot\text{H}_2\text{O}$ at the molar ratio of 1:1.03. The mixture was then calcined at different temperatures from 500 to 900 °C for 12 h under an oxygen atmosphere. The products are named NM91-X (X stands for temperature). The B-doped NM91 sample was synthesized by adding 0.5 mol% B_2O_3 into the grinding process, followed by calcination at 770 °C for 12 h under an oxygen atmosphere.

Materials Characterization

The cathode crystal structure was analyzed by X-ray diffraction (Rigaku, D/max-2550) using $\text{Cu K}\alpha$ radiation in the 2θ range of 5-130° with a 0.02° step size. The lattice parameters and the Li/Ni mixing degree were obtained from XRD data by Rietveld refinement using Fullprof software. In-situ XRD patterns were collected on high-resolution X-ray diffractometer (Empyrean, PANalytical). Scanning electron microscopy (SEM, Zeiss Merlin Compact) was used for morphological characterization. The samples for cross-sectional SEM analysis were prepared by ion beam slope cutter (Leica EM TIC 3X). Transmission electron microscopy (TEM, JEM-2100F) and scanning transmission electron microscopy (STEM, Hitachi S-5500) were used to investigate the microstructure of cathodes. The cathode samples for TEM and STEM analysis were prepared using the focused ion beam (FIB, Zeiss Crossbeam 340). The cycled cathode was investigated by X-ray photoelectron spectroscopy (XPS, Thermofisher Escalab 250XI), and the standard C 1s peak (284.8 eV) was used to calibrate the whole spectrum of the sample. For gas generation analysis, in operando differential electrochemical mass spectrometry (DEMS) was conducted by mass spectrometer

(Shanghai Linglush QMG220). The cells for DEMS analysis were cycled to 4.7 V versus Li^+/Li at 0.1 C (1 C = 190 mA g^{-1}). TGA-DSC measurement was conducted through a TGA/DSC system (Mettler Toledo, STAR System) at a heating rate of 10 $^{\circ}\text{C min}^{-1}$ under air flow. The mechanical property was measured through nanoindentation (G200, Keysight technologie) under a maximum of 18 mN in load.

Electrochemical Measurements

The cathode was prepared by mixing the NM91-X powder, polyvinylidene fluoride (PVDF) binder, and carbon black additive with a mass ratio of 8:1:1 in N-methyl-2-pyrrolidone (NMP) solvent and drying at 80 $^{\circ}\text{C}$ under vacuum for 12 h. The full cells were assembled with a lithium disk as anode and a Celgard 2325 separator into CR-2025 coin cell cases in a glovebox under an inert atmosphere. The loading of the cathode is approximately 4 mg/cm^2 . The electrolyte was 1 mol L^{-1} LiPF_6 dissolved in ethylene carbonate (EC) and dimethyl carbonate (DMC) (EC: DMC = 3:7 by volume) with 2% vinylene carbonate (VC). The cells were cycled at various C-rates and cutoff voltages (3.0-4.3 V and 3.0-4.4 V, versus Li^+/Li). After cycling, the cells were disassembled in a glove box under an inert atmosphere. The cathode was then washed with DMC to remove residual electrolyte before characterization. Electrochemical impedance spectroscopy was conducted from 1 MHz to 10 mHz with an applied AC potential amplitude of 10 mV. The galvanostatic intermittent titration technique (GITT) was used to test the lithium ion diffusion coefficient, and all samples data were measured with a galvanostatic current set to 0.1 C, the charge or discharge process for 20 min, and a time interval of 60 min close to steady state.

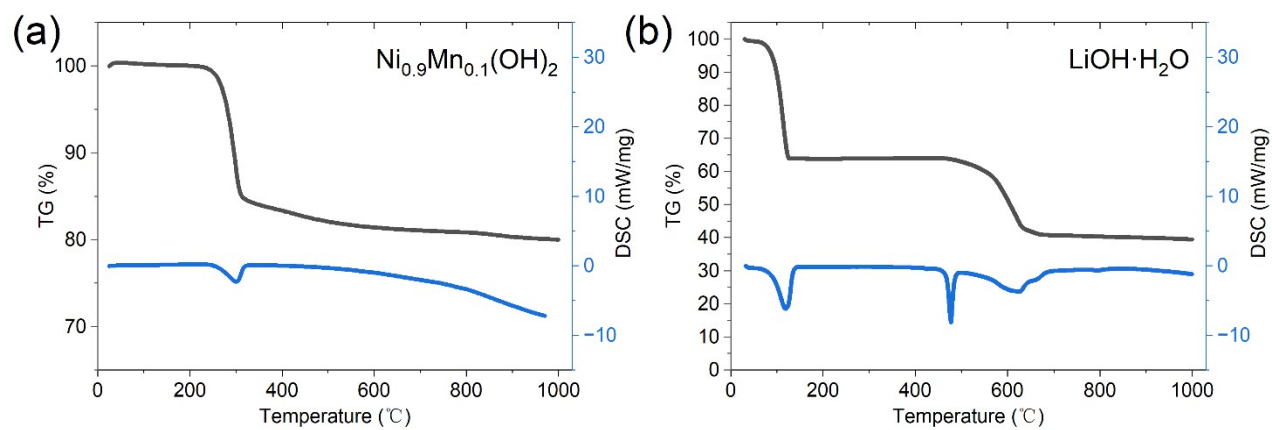


Figure S1. Thermogravimetric analysis and differential scanning calorimetry (TGA-DSC) curve of (a)

$\text{Ni}_{0.9}\text{Mn}_{0.1}(\text{OH})_2$ and, (b) $\text{LiOH}\cdot\text{H}_2\text{O}$, respectively.

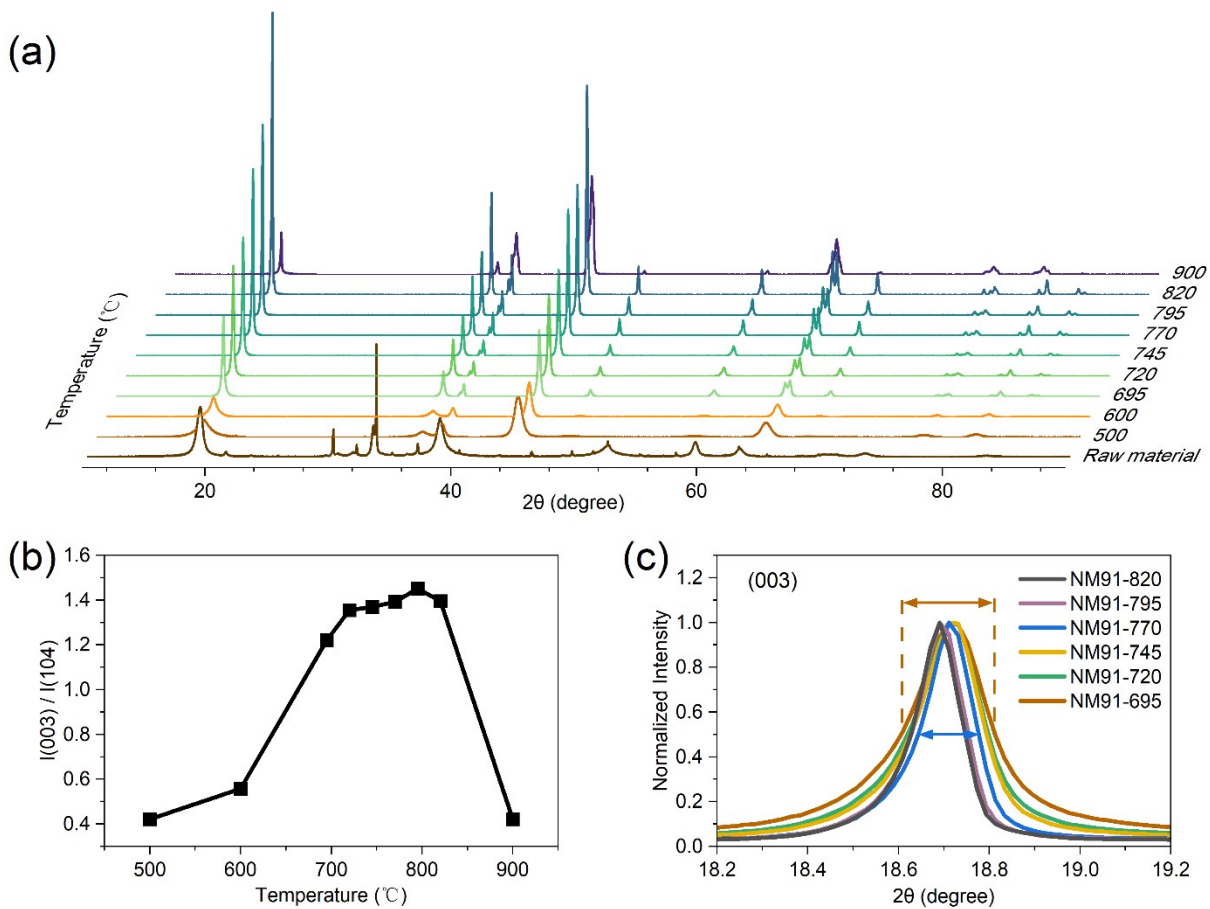


Figure S2. (a) Ex-situ XRD patterns of raw material before calcination and NM91-500 to NM91-900 samples. (b) The ratio of the intensity of (003) and (104) reflections NM91 from 500°C to 900°C extracted from the ex-situ XRD patterns in Figure S2(a). (c) Normalized (003) reflection for NM91-695 to NM91-820.

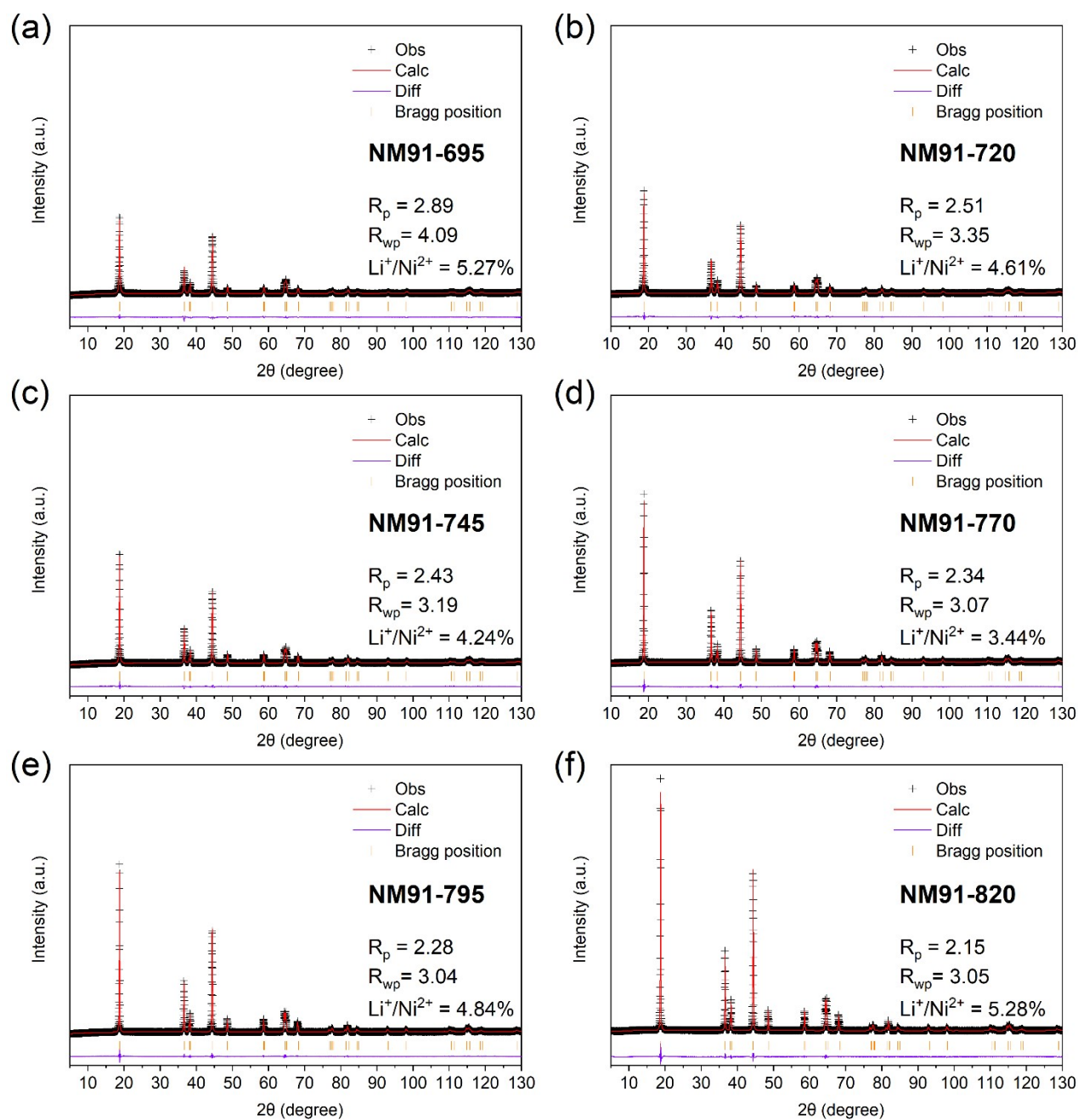


Figure S3. Rietveld refinement results of (a) NM91-695, (b) NM91-720, (c) NM91-745, (d) NM91-770, (e) NM91-795, and (f) NM91-820.



Figure S4. The SEM images of (a) precursor, (b) NM91-500 and, (c) NM91-600.

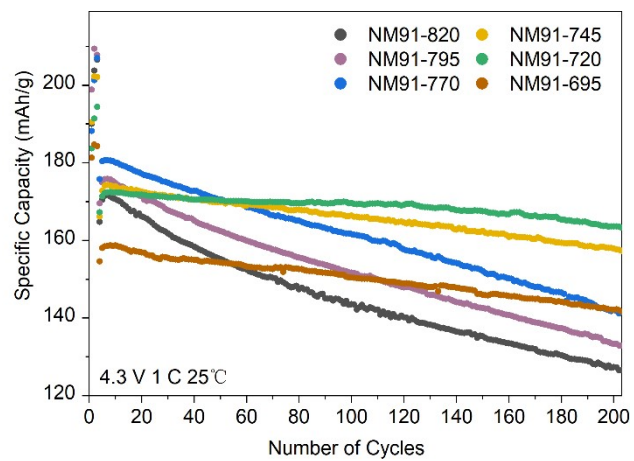


Figure S5. Cycling performances at a rate of 1 C with respect to the number of cycles.

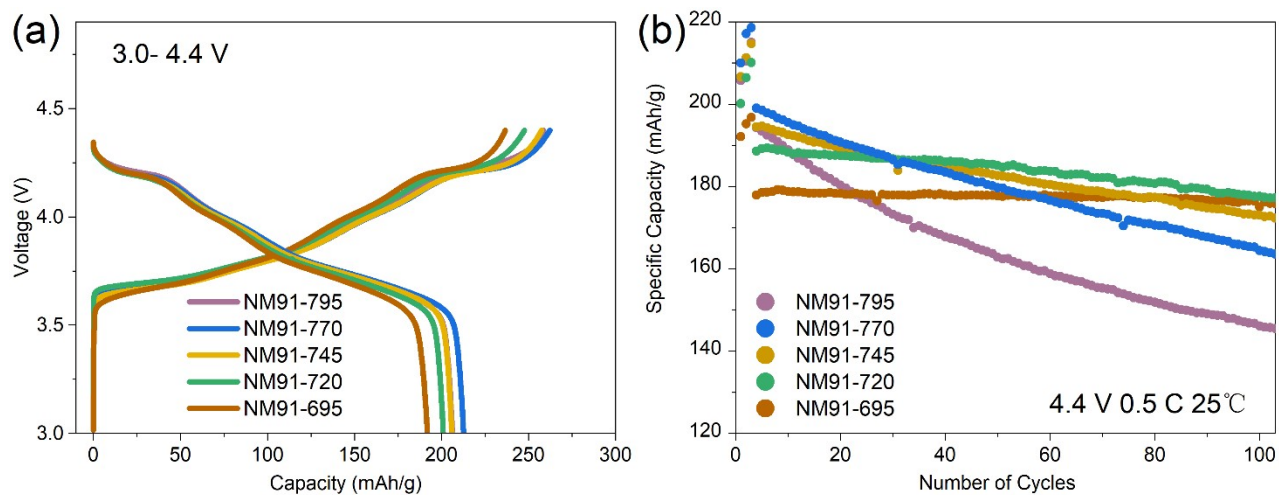


Figure S6. (a) Initial charge and discharge curves at 0.1 C, for cycling between 3.0 and 4.4 V for NM91-695 to NM91-795 cathodes. (b) Cycling performances at 0.5 C with respect to the number of cycles.

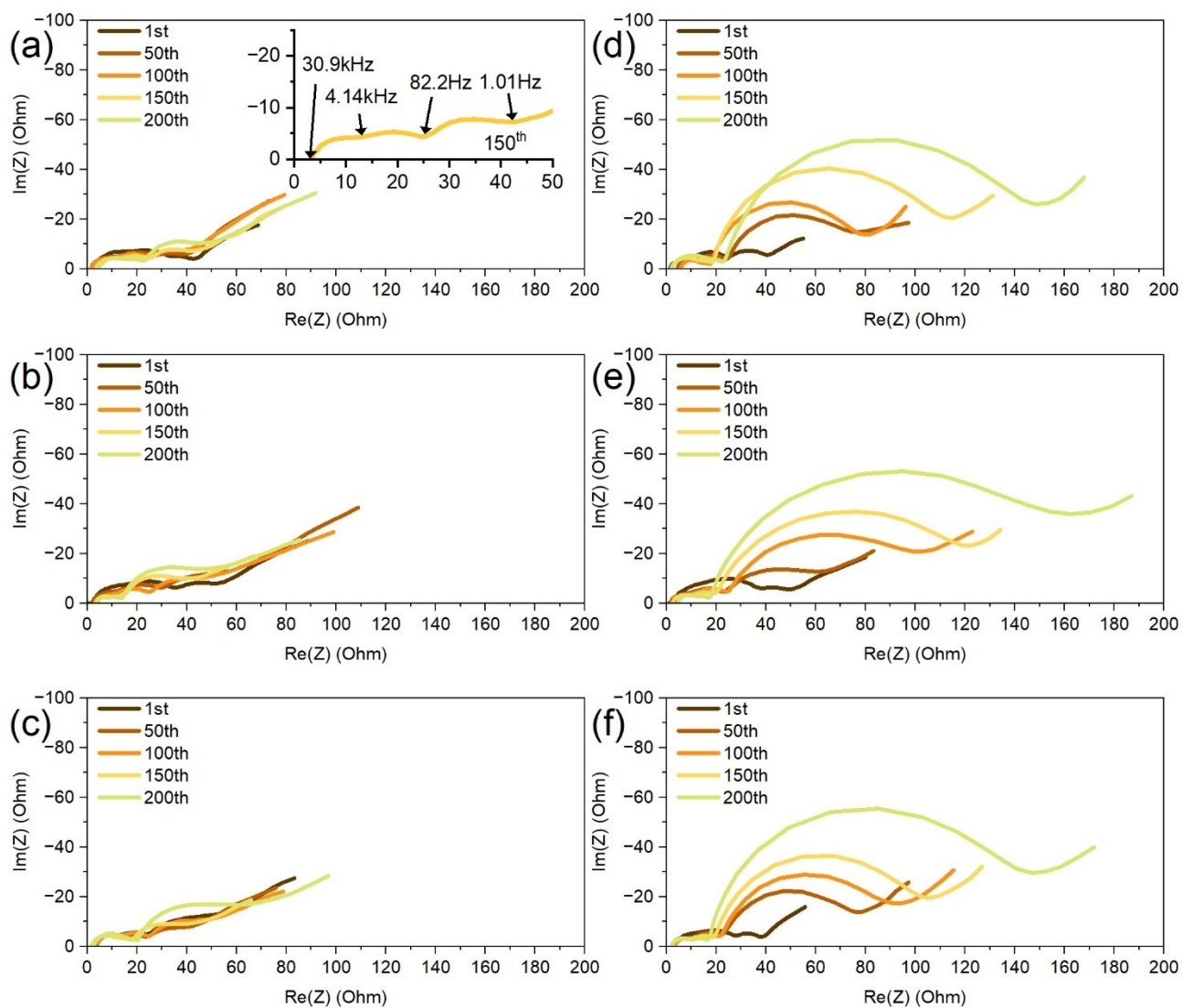


Figure S7. Nyquist plots of the electrochemical impedances measured at 4.3 V at every 50th cycle for (a) NM91-695 (**Inset:** Enlarged curve at 150th cycle for instance), (b) NM91-720, (c) NM91-745, (d) NM91-770, (e) NM91-795, and (f) NM91-820.

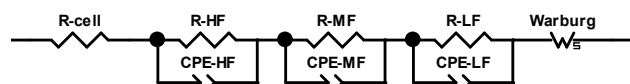


Figure S8. Corresponding equivalent circuit model for Nyquist plots analysis in Figure S7.

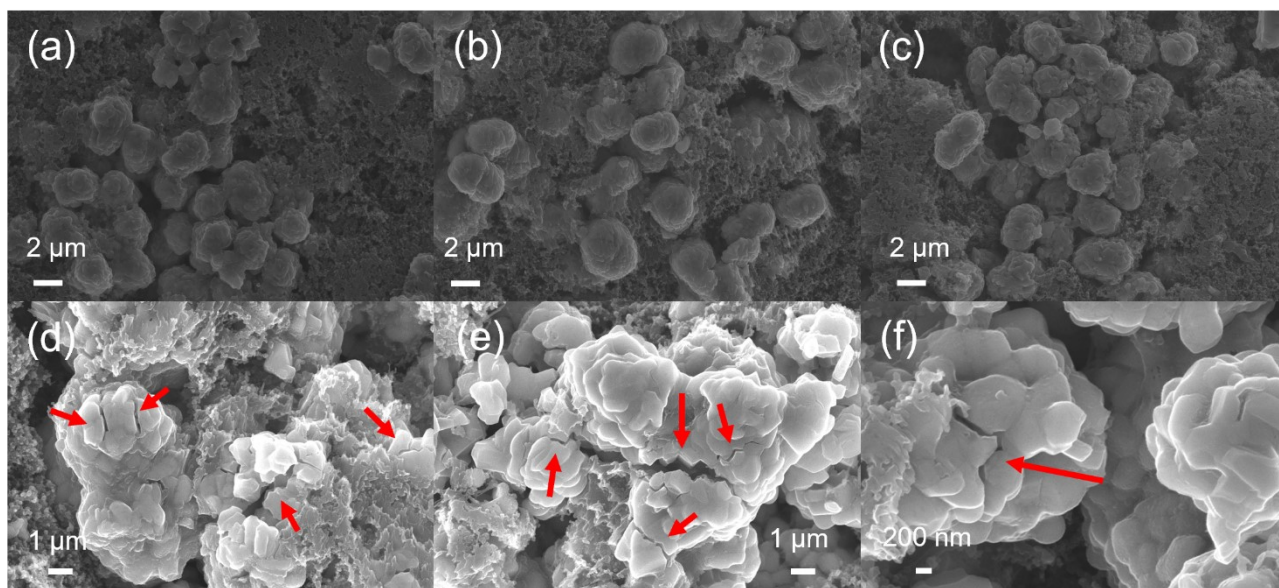


Figure S9. The SEM images for (a) NM91-695, (b) NM91-720, (c) NM91-745, (d) NM91-770, (e) NM91-795, and (f) NM91-820, on the cathode side after 200 cycles at 3.0-4.3 V (red arrows are noted for cracks).

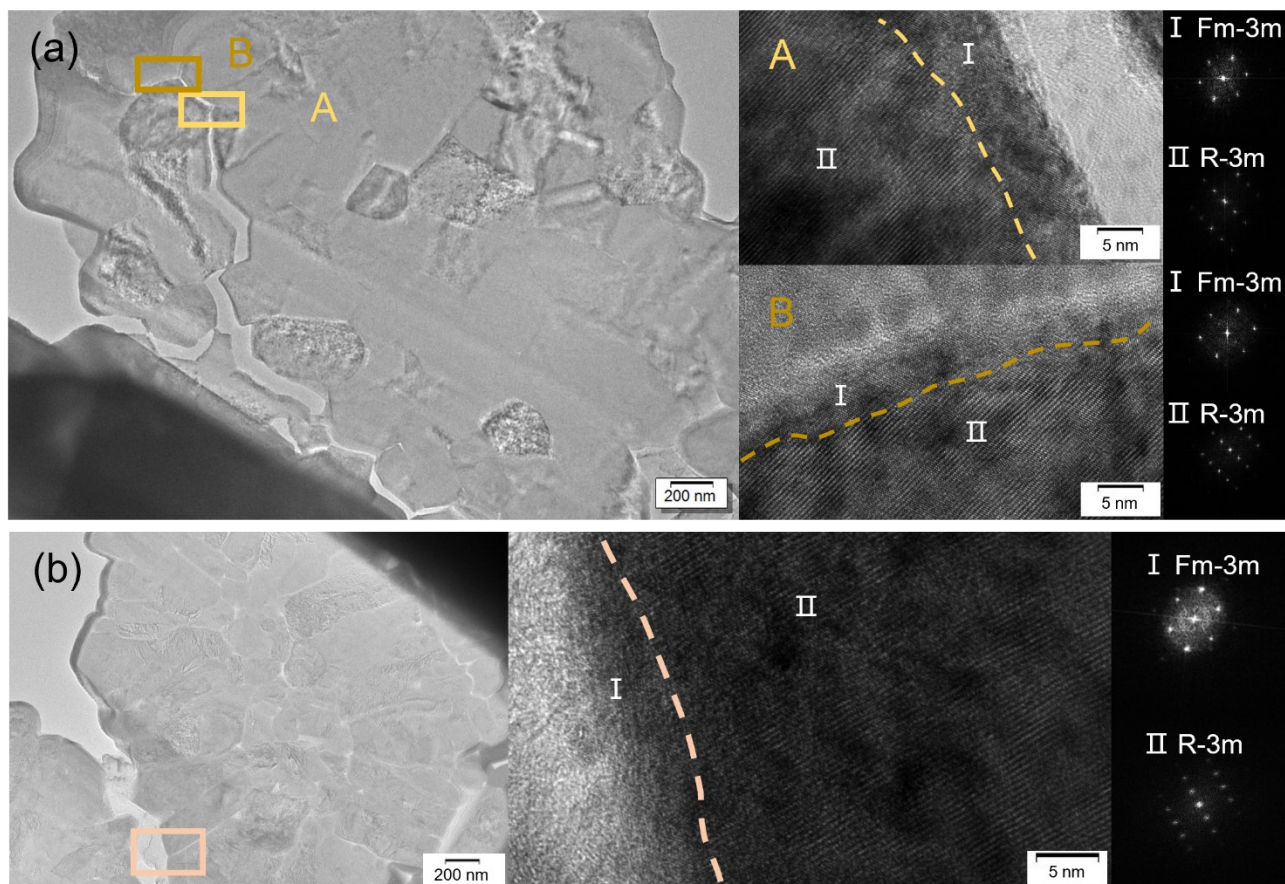


Figure S10. The TEM photos and the corresponding FFT for (a) NM91-770 after 100 cycles, (b) NM91-720 after 100 cycles.

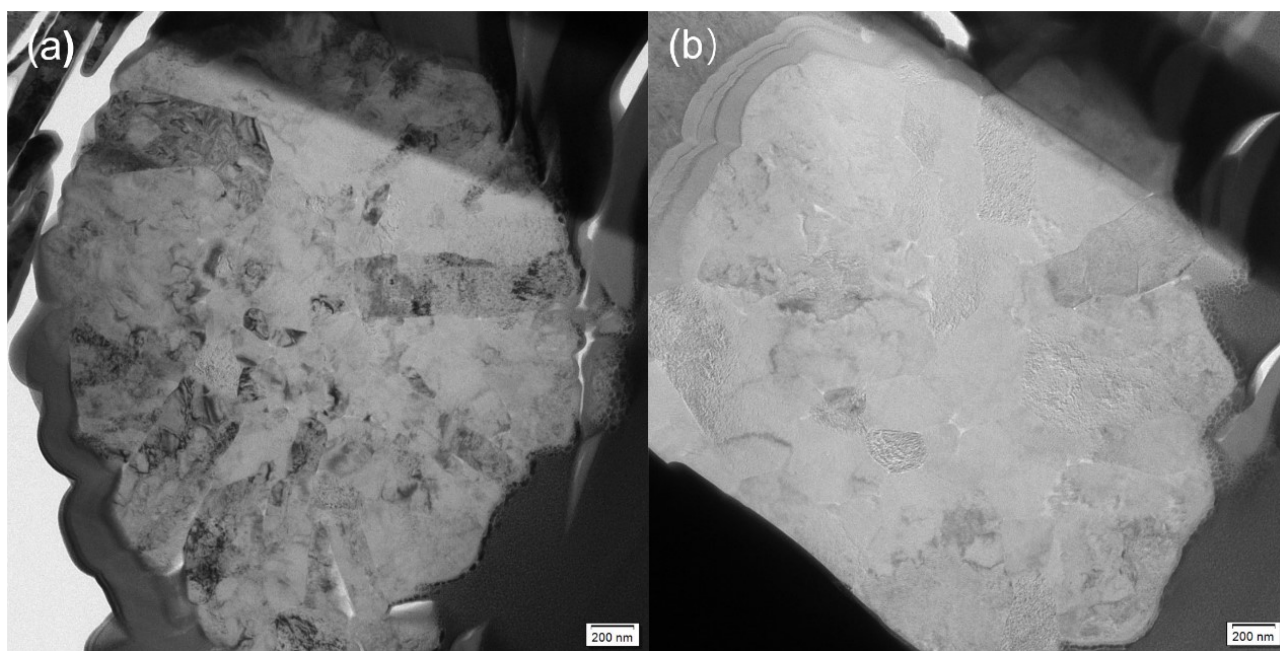


Figure S11. Pristine cathode particle under TEM analysis after FIB for NM91-720 and NM91-770.

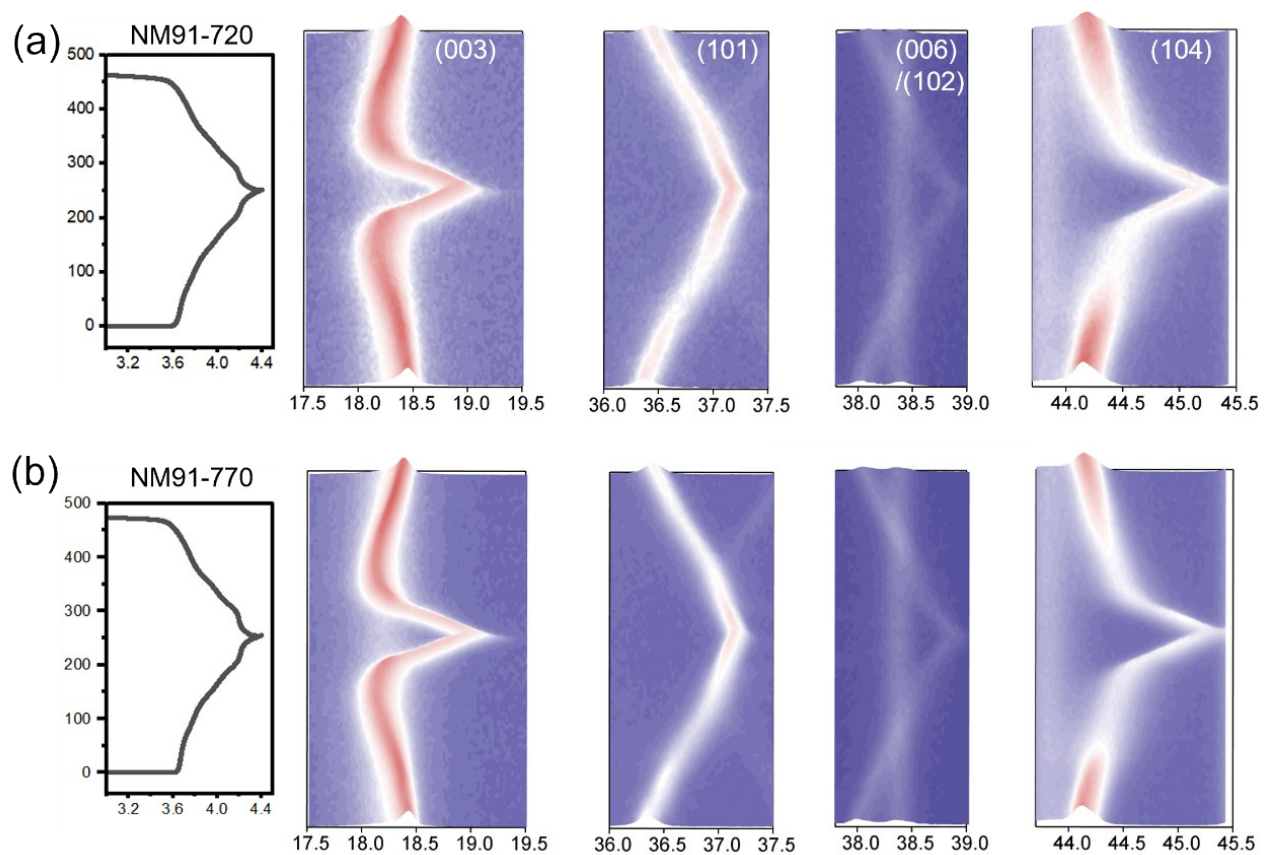


Figure S12. In-situ XRD analysis for (a) NM91-720, and (b) NM91-770 with corresponding charge-discharge curve from 3.0 to 4.4 V at 0.1 C.

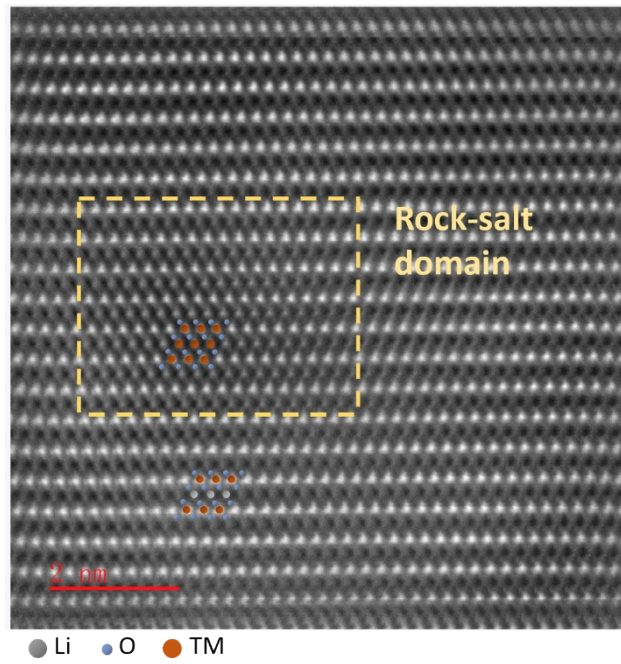


Figure S13. HADDF-STEM image of the rock-salt domain in the bulk of NM91-720.

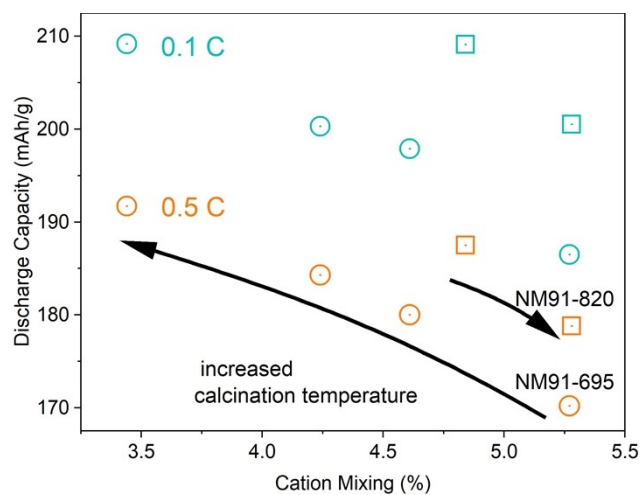


Figure S14. The discharge capacity of different rate (0.1 C and 0.5 C) with the respect to cation mixing degree. NM91-695 to NM91-770 were labeled as circle, NM91-795 to NM91-820 were labeled as square. Note that the capacity of the third cycle at 0.1 C was chosen to avoid the insufficient side reaction.

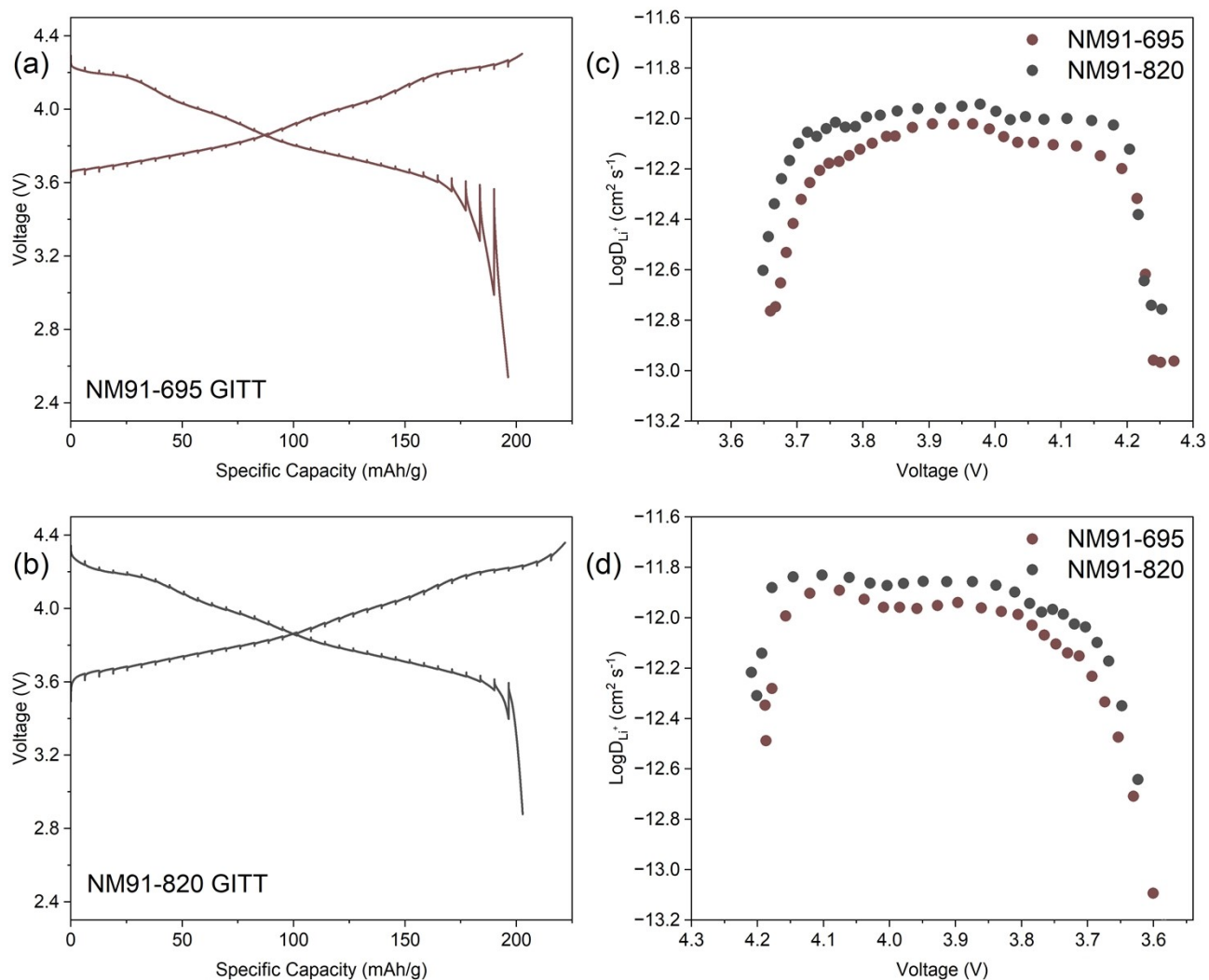


Figure S15. The charge-discharge profiles of (a) NM91-695 and (b) NM91-820 from GITT tests. The calculated D_{Li^+} based on GITT results upon (c) charging and (d) discharging process.

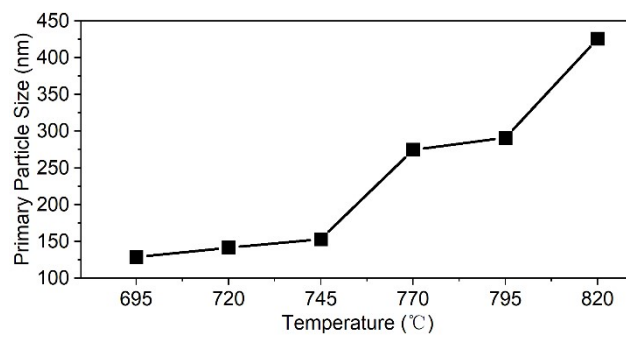


Figure S16. The size of primary particles with the respect to calcination temperature.

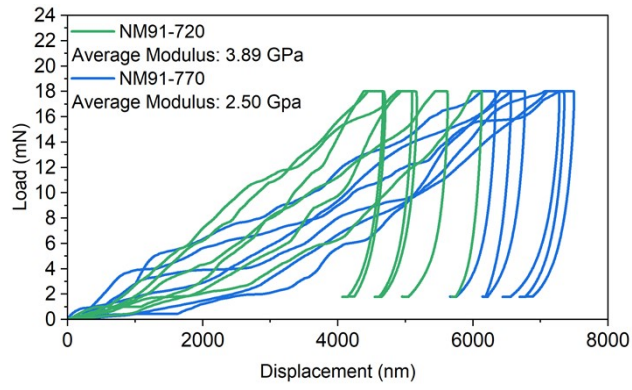


Figure S17. Force-displacement curves for NM91-720 and NM91-770 via nanoindentation approach.

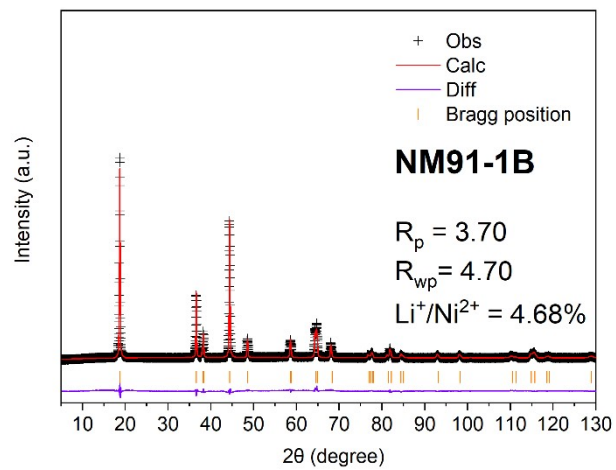


Figure S18. Rietveld refinement results of NM91-1B.

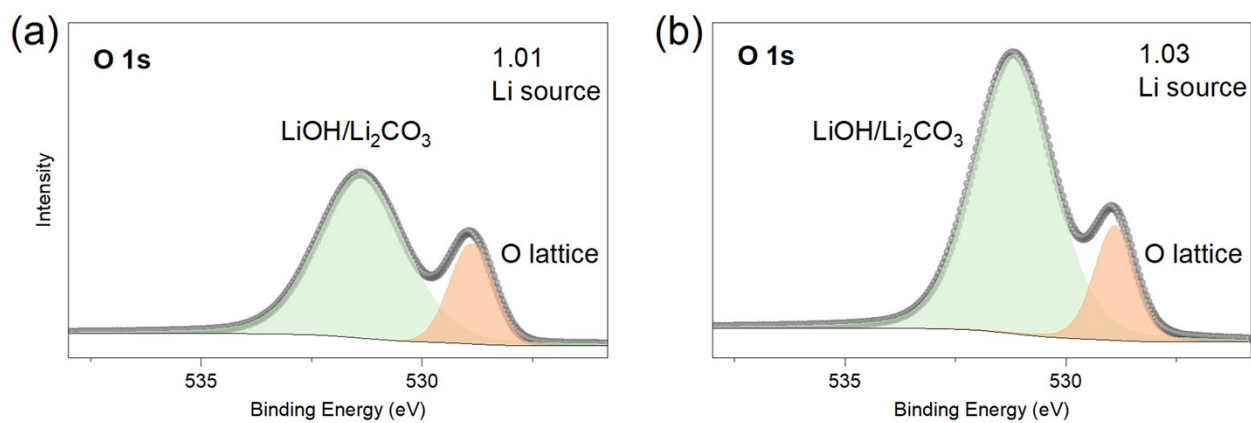


Figure S19. XPS spectra of O 1s peaks of pristine NM91-770 with (a) 1% excess Li source and (b) 3% excess Li source.

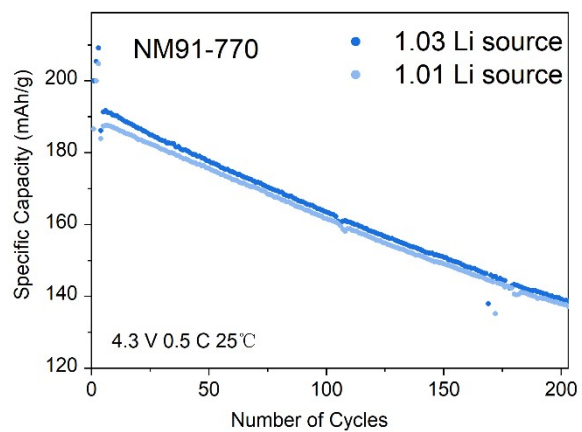


Figure S20. Cycling performances at 0.5 C of NM91-770 with different amount of Li source.

Table S1. Rietveld refinements of the XRD patterns for NM-X cathodes

NM91-695	atom	site	X	Y	Z	Occ
a = 2.8752 Å	Li	3a	0	0	0	0.0789
c = 14.1990 Å	Ni	3a	0	0	0	0.0044
Volume = 101.7 Å ³	Ni	3b	0	0	0.5	0.0706
Rp = 2.89	Mn	3b	0	0	0.5	0.0083
Rwp = 4.09	Li	3b	0	0	0.5	0.0044
Li/Ni = 5.27%	O	6c	0	0	0.2422	0.1667
NM91-720	atom	site	X	Y	Z	Occ
a = 2.8750 Å	Li	3a	0	0	0	0.0795
c = 14.2034 Å	Ni	3a	0	0	0	0.0039
Volume = 101.7 Å ³	Ni	3b	0	0	0.5	0.0712
Rp = 2.51	Mn	3b	0	0	0.5	0.0083
Rwp = 3.35	Li	3b	0	0	0.5	0.0039
Li/Ni = 4.61%	O	6c	0	0	0.2416	0.1667
NM91-745	atom	site	X	Y	Z	Occ
a = 2.8752 Å	Li	3a	0	0	0	0.0798
c = 14.2054 Å	Ni	3a	0	0	0	0.0035
Volume = 101.7 Å ³	Ni	3b	0	0	0.5	0.0715
Rp = 2.43	Mn	3b	0	0	0.5	0.0083
Rwp = 3.19	Li	3b	0	0	0.5	0.0035
Li/Ni = 4.24%	O	6c	0	0	0.2417	0.1667
NM91-770	atom	site	X	Y	Z	Occ
a = 2.8760 Å	Li	3a	0	0	0	0.0805
c = 14.2081 Å	Ni	3a	0	0	0	0.0029
Volume: 101.8 Å ³	Ni	3b	0	0	0.5	0.0721
Rp = 2.34	Mn	3b	0	0	0.5	0.0083
Rwp = 3.07	Li	3b	0	0	0.5	0.0029
Li/Ni: 3.44%	O	6c	0	0	0.2418	0.1667
NM91-795	atom	site	X	Y	Z	Occ
a = 2.8793 Å	Li	3a	0	0	0	0.0793
c = 14.2165 Å	Ni	3a	0	0	0	0.0040
Volume = 102.1 Å ³	Ni	3b	0	0	0.5	0.0710
Rp = 2.28	Mn	3b	0	0	0.5	0.0083
Rwp = 3.04	Li	3b	0	0	0.5	0.0040

Li/Ni = 4.84%	O	6c	0	0	0.2420	0.1667
NM91-820	atom	site	X	Y	Z	Occ
a = 2.8808 Å	Li	3a	0	0	0	0.0789
c = 14.2203 Å	Ni	3a	0	0	0	0.0044
Volume = 102.2 Å ³	Ni	3b	0	0	0.5	0.0706
Rp = 2.15	Mn	3b	0	0	0.5	0.0083
Rwp = 3.05	Li	3b	0	0	0.5	0.0044
Li/Ni = 5.28%	O	6c	0	0	0.2420	0.1667

Table S2. Rietveld refinements of the XRD patterns for B-doped cathode

NM91-1B	atom	site	X	Y	Z	Occ
a = 2.8782 Å	Li	3a	0	0	0	0.0794
c = 14.2125 Å	Ni	3a	0	0	0	0.0039
Volume = 102.0 Å ³	Ni	3b	0	0	0.5	0.0711
Rp = 3.70	Mn	3b	0	0	0.5	0.0083
Rwp = 4.70	Li	3b	0	0	0.5	0.0039
Li/Ni = 4.68%	O	6c	0	0	0.2423	0.1667